

Assessing Treatment Response of Glioblastoma to an HDAC Inhibitor Using Whole-Brain Spectroscopic MRI

Saumya S. Gurbani^{1,2}, Younghyun Yoon¹, Brent D. Weinberg³, Eric Salgado¹, Robert H. Press¹, J. Scott Cordova¹, Karthik K. Ramesh^{1,2}, Zhongxing Liang¹, Jose Velazquez Vega⁴, Alfredo Voloschin⁵, Jeffrey J. Olson⁶, Eduard Schreiber¹, Hyunsuk Shim^{1,2,3}, and Hui-Kuo G. Shu¹

¹Department of Radiation Oncology, Winship Cancer Institute of Emory University, Atlanta, GA; ²Department of Biomedical Engineering, Emory University and Georgia Institute of Technology, Atlanta, GA; Departments of ³Radiology and Imaging Sciences, ⁴Pathology and Laboratory Medicine; ⁵Hematology and Medical Oncology, and ⁶Neurosurgery, Emory University School of Medicine, Atlanta, GA

Corresponding Authors:

Hyunsuk Shim, PhD

Department of Radiation Oncology, Winship Cancer Institute of Emory University, 1701 Uppergate Drive, Atlanta, GA 30322;

E-mail: hshim@emory.edu; and Hui-Kuo Shu,

E-mail: hshu@emory.edu

Key Words: glioblastoma, spectroscopic MRI, histone deacetylase inhibitor, belinostat, orthotopic rat glioma model

Abbreviations: Histone deacetylase inhibitors (HDACi), glioblastoma (GBM), progression-free survival (PFS), radiation therapy (RT), temozolomide (TMZ), histone deacetylases (HDACs), suberanilohydroxamic acid (SAHA), spectroscopic magnetic resonance imaging (sMRI), myo-inositol (MI), myo-inositol phosphatase (MIP), dimethyl sulfoxide (DMSO), Dulbecco's modified eagle medium (DMEM), lipopolysaccharide (LPS), echo planar spectroscopic imaging (EPSI), T1-weighted (T1w), Inventory of Depressive Symptomatology Self Report (IDS-SR)

ABSTRACT

Histone deacetylases regulate a wide variety of cellular functions and have been implicated in redifferentiation of various tumors. Histone deacetylase inhibitors (HDACi) are potential pharmacologic agents to improve outcomes for patients with gliomas. We assessed the therapeutic efficacy of belinostat (PXD-101), an HDACi with blood–brain barrier permeability. Belinostat was first tested in an orthotopic rat glioma model to assess *in vivo* tumoricidal effect. Our results showed that belinostat was effective in reducing tumor volume in the orthotopic rat glioma model in a dose-dependent manner. We also tested the antidepressant activity of belinostat in 2 animal models of depression and found it to be effective. Furthermore, we confirmed that myo-inositol levels improved by belinostat treatment *in vitro*. In a human pilot study, it was observed that belinostat in combination with chemoradiation may delay initial recurrence of disease. Excitingly, belinostat significantly improved depressive symptoms in patients with glioblastoma compared with control subjects. Finally, spectroscopic magnetic resonance imaging of 2 patient cases from this pilot study are presented to indicate how spectroscopic magnetic resonance imaging can be used to monitor metabolite response and assess treatment effect on whole brain. This study highlights the potential of belinostat to be a synergistic therapeutic agent in the treatment of gliomas.

INTRODUCTION

Glioblastomas (GBMs; WHO grade IV glioma) are highly aggressive malignant primary adult brain tumors. Despite comprehensive treatment consisting of neurosurgical resection, high-dose radiation therapy (RT), and chemotherapy (temozolomide, TMZ), the median progression-free survival (PFS) remains 5–7 months (1). Given these poor results, there is an urgent need for improved therapy options. A potential therapeutic target is the family of histone deacetylases (HDACs) that comprises 18 different nuclear and cytoplasmic proteins primarily involved in modulating gene expression through epigenetic mechanisms but also having a broad impact on many additional pathways, including ones associated with cellular metabolism and cell cycle regulation (2–4). Several specific HDACs, particularly in class I and class II, show increased expression and are thought to

contribute to oncogenesis in several types of cancer, including ones arising in breast, prostate, lung, and brain (5). As a result, the development of targeted HDAC inhibitors (HDACi) is an active research area for pharmacologic treatment of these diseases (6). In 2006, suberanilohydroxamic acid (SAHA), a first-generation HDACi which targets multiple class I and class II HDAC family members, became the first HDACi to receive FDA approval for advanced cutaneous T cell lymphomas (7). Preclinical investigations of SAHA have also shown antitumor effects in orthotopic glioma animal models (8, 9). This suggests that development of potent HDACis capable of penetrating the blood–brain barrier has the potential to improve therapeutic outcomes of patients with GBM. Research is ongoing into evaluating the synergistic effect of HDACi and chemoradiation for such patients (10).

Belinostat (PXD101, Spectrum Pharmaceuticals Inc., Irvine, CA), a new pan-HDACi that is structurally similar to SAHA, improves upon the former by having greater blood–brain barrier uptake, which may potentiate its use in the treatment of CNS tumors (11, 12). Belinostat received FDA approval for patients with relapsed/refractory peripheral T cell lymphoma in 2014 (13). In this work, we seek to show a translational analysis of belinostat in the treatment of GBM and describe how a quantitative imaging technique, proton spectroscopic magnetic resonance imaging (sMRI), can serve as a reliable imaging biomarker for monitoring therapy response of belinostat when combined with standard chemoradiation. First, we tested the antitumor effect of belinostat in an orthotopic rat glioma model. Second, we assessed the antidepressant effect of belinostat in 2 well-known depression animal models. We also quantified the increase of mRNA levels of bottleneck enzymes for the production of myo-inositol (MI), myo-inositol phosphatase (MIP), an sMRI-detectable metabolite known to be associated with depression. Finally, we assessed the impact of belinostat in combination with chemoradiation in a human pilot study (ClinicalTrials.gov ID: NCT02137759) and present interim results for PFS and a survey of depressive symptomatology. We present sMRI and clinical data from patients in this study to evaluate the modality's use in monitoring response to belinostat + chemoradiation. Our results show a statistically significant improvement of depressive symptoms with belinostat treatment, consistent with our animal data. These results support the utility of belinostat as an adjuvant therapy for GBM and sMRI as a quantitative imaging technique that can noninvasively monitor therapy response.

METHODOLOGY

Cell Culture and In Vitro HDACi Treatment

Belinostat and other HDACis were dissolved in dimethyl sulfoxide (DMSO) to obtain a 100mM stock solution. A 9L rat glioma cell line was maintained in Dulbecco's modified eagle medium (DMEM) (Mediatech Inc., Manassas, MA) supplemented with 10% fetal bovine serum and antibiotics at 37°C in 5% CO₂. 9L cells were plated in 100-mm cell culture petri dishes. Cells were then treated 2 days following seeding with fresh medium containing various HDACis at concentrations of 1 μM for 12 h and were collected to prepare total RNA.

RNA Isolation, RT-PCR, and Real-Time RT-PCR

Cells were collected 12-hour postincubation; these cells underwent RNA isolation and reverse transcription-polymerase chain reaction (RT-PCR) to assess the total mRNA expression levels of the key enzymes in the synthesis of MI (MIP) (8). Total RNA was extracted from cultured cells following the manufacturer's instructions as previously described (14). Primer sequences of MIP-1 were as follows: MIP-1 (GenBank accession number: NM_016368), 5'-AGCTGCATCGAGAACATCCT-3' and 5'-GGGTACCGTCTTTCTTGT-3'; SYBR Green quantitative PCR reaction was carried out in a 15-μL reaction volume containing 2× PCR Master Mix (Applied Biosystems) per our previous reports (14).

Antitumor Effect in an In Vivo Rat Glioma Model

Using a previously described orthotopic rat glioma model (8), the tumoricidal and psychological effects of belinostat were

tested. 9L rat glioma cells were stereotactically injected into the frontal lobes of male Fischer 344 rats (n = 9). At postinjection day 9, rats were treated with a daily intraperitoneal injection of either vehicle (10% DMSO, n = 1) or tiered doses of belinostat (n = 2 each of 25 mg/kg, 50 mg/kg, 75 mg/kg, and 100 mg/kg) for 4 days. Throughout the experiment, rats were monitored for mood behavior and activity levels using the volume of droppings as a surrogate measurement. Animals were sacrificed on postinjection day 12, and tumors were excised. This protocol was approved by the Institutional Animal Care and Use Committee (IACUC) at Emory University.

Antidepressant Effect Assessment of Belinostat in 2 Animal Models

As described previously (15), the forced-swim test and tail suspension tests were used to assess the antidepressant effect of belinostat. Five 6-week-old C57 black female mice were used in each group for forced-swim test and five 7-week-old NIH Swiss male mice were used in each group for tail suspension test. C57 black mice may not perform well in the tail suspension test owing to tail climbing behavior (<https://www.research.psu.edu/arp/experimental-guidelines/rodent-behavioral-tests-1/rodent-behavioral-tests.html>), whereas the NIH Swiss mice did not have similar issues. The forced-swim test was performed 6 h after belinostat treatment (75 mg/kg i.p.) in a 4-L beaker containing 3 L of tap water at a temperature of 25°C. Video tracking-based methods were used to record the duration of time spent “immobile” in the arena over 6 minutes (immobility measured between 2 and 8 minutes of a 10-minute trial; the extent of immobility correlates with levels of depression). Similarly, the tail suspension test is based on the fact that animals subjected to inescapable stress of being suspended by their tail for the short term, would develop an immobile posture (16). For the tail suspension test, the lipopolysaccharide (LPS)-induced depression model was used (17). Twenty-four hours after LPS administration (Sigma L3129; 0.85 mg/kg i.p.), the tail suspension test was performed. Video tracking-based methods were used to record the duration of time spent in immobility for 6 minutes.

Clinical Study

Patients with newly diagnosed GBM were enrolled in either the control or treatment arm of an Institutional Review Board (IRB)-approved clinical trial at Emory University (ClinicalTrials.gov ID NCT02137759), wherein the treatment arm received intravenous belinostat (Spectrum Pharmaceuticals, Irvine, CA) as an investigational therapeutic. The study was not randomized, with patients serially enrolling into the control arm (in 2014–2015) followed by the belinostat treatment arm (in 2015–2018). All patients underwent maximal safe tumor resection, if resection was feasible, before enrolling in the study. Patients in both arms of the trial received standard-of-care therapy consisting of daily TMZ (75 mg/m²) × 42 days and focal radiation doses of 60 and 51 Gy to the resection cavity/residual contrast-enhancing tissue (per T1-weighted contrast-enhanced MRI postresection) and T2/FLAIR signal, respectively, in 30 fractions. Margins of 0.5–1.0 cm and 0.3–0.5 cm were added to the target volumes to generate the clinical treatment volume and planning treatment volume to account for microscopic disease spread and spatial uncertainty

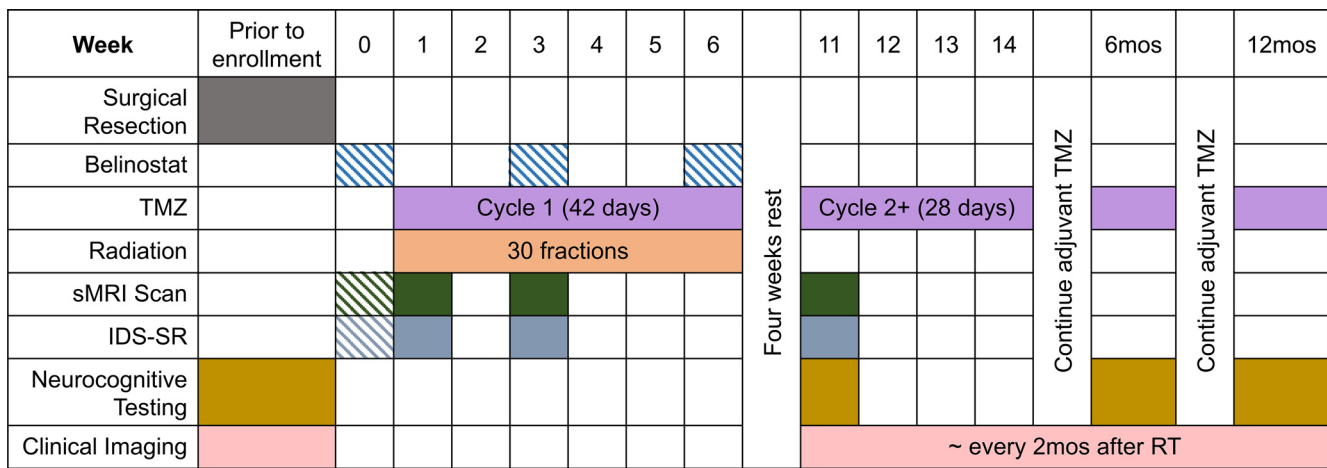


Figure 1. One-year timeline of chemotherapy, intravenous belinostat, radiation, spectroscopic magnetic resonance imaging (sMRI) scanning, Inventory of Depressive Symptomatology Self Report (IDS-SR) survey, and neurocognitive testing for patients in NCT02137759. Hashed boxes indicate items conducted for patients in only the treatment arm of the study.

in treatment delivery (18). In the treatment arm, patients received daily intravenous doses of belinostat at either 500 or 750 mg/m² for 5 consecutive days in 3 cycles, spaced 3 weeks apart beginning 1 week before the start of chemoradiation, as shown in Figure 1. The first 3 patients received a higher dose of belinostat. However, because 2 of the patients had serious adverse events with hematologic toxicity during the course of belinostat, TMZ, and radiation, the dose was lowered to 500 mg/m² for the remaining patients in the trial.

Each patient in the study underwent an sMRI scan prior to starting chemoradiation (week 1), after 2 weeks of chemoradiation (week 3), and 4 weeks after completing radiation (week 11). Patients in the treatment arm underwent an additional sMRI scan before starting the first week of belinostat (week 0). sMRI scans were conducted on a 3 T MR scanner (Siemens TimTrio or Siemens PRISMA with 32 channel head coil, Siemens Healthineers, Erlangen, Germany) using an echo planar spectroscopic imaging (EPSI) sequence combined with generalized autocalibrating partially parallel acquisition (GRAPPA), and metabolite maps were produced using the MIDAS software (University of Miami, Miami, FL) (19, 20). The metabolite maps were coregistered to a volumetric T1-weighted (T1w) MRI taken during the same scanning session with the patient in the same orientation. Longitudinal scans on the 4 patients were coregistered and brought into the first scan (week 0/1) imaging space using rigid registration. After each sMRI scan, the patient completed the Inventory of Depressive Symptomatology Self Report (IDS-SR), a validated 30-question survey designed to assess depressive symptoms (21, 22).

EPSI/GRAPPA sequence parameters were optimized to enhance the signal of choline (Cho, a metabolite involved in the synthesis of the phospholipid cell membrane and increased in tumors) and NAA (a healthy neuronal marker decreased as neoplasia invades into and destroys neuronal tissue). Patients were followed-up with standard-of-care imaging (contrast-enhanced T1-weighted MRI, CE-T1w MRI; fluid attenuation

inversion recovery, FLAIR) for 12 months post-treatment or until progression of disease was confirmed by neuroradiologist. A total of 26 patients (13 control, 13 treatment) were enrolled at Emory University; of these, 3 did not complete the treatment protocol (1 in control arm, 2 in belinostat arm), and 2 did not undergo surgical resection of tumor (only underwent a biopsy for diagnosis). These 5 patients are excluded from analysis (see online Supplemental Figure 1). PFS is reported for patients based on time to radiologic confirmation of disease progression (per CE-T1w MRI) from the date of surgery. Data are right-censored for patients who have no known disease progression or were lost to follow-up. Sample cases from each arm of the study are shown to show the ability of sMRI to identify early response to treatment. Because follow-up data are continuing to be collected for patients in the treatment arm of the study, statistical analyses of the full data will be presented in future work.

RESULTS

Antitumor Effect of Belinostat in an Orthotopic Rat Model

In Figure 2, photographs of the 9 rats evaluated in this experiment are shown in their cage at pretreatment with belinostat and at day 13, 4 days after treatment, when the rats were sacrificed. The volume of animal droppings seen in the cage is used as a surrogate measure of activity and normal physiology. Rats showed decreased movement and grooming, measures of mood, before treatment with belinostat. The restoration of activity and improved mood was observed in a dose-dependent manner, with normal levels observed in rats treated with the highest 2 doses (75 mg/kg and 100 mg/kg). Photographs of the tumor in situ and excised are also shown in Figure 2, showing a similar dose-dependent decrease in tumor volume from untreated mice through the increasing doses of belinostat.

Figure 2. A rat model of stereotactically injected 9L glioma cells shows a dose-dependent response in both tumor volume and mood/activity levels when treated with belinostat.

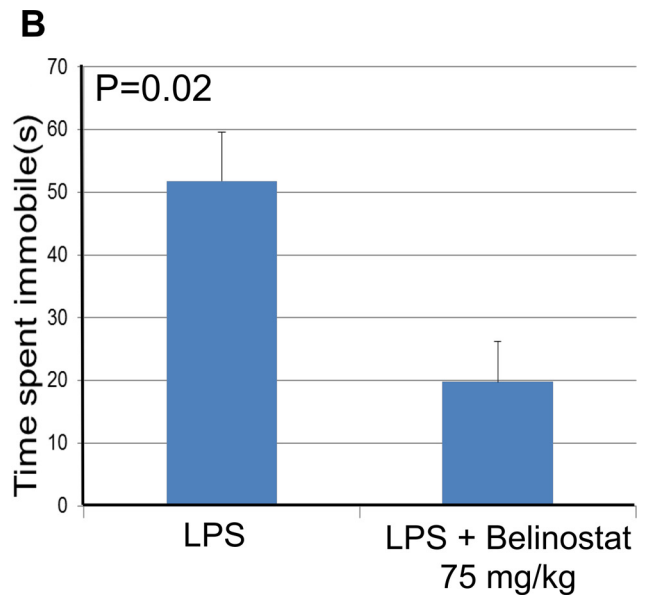
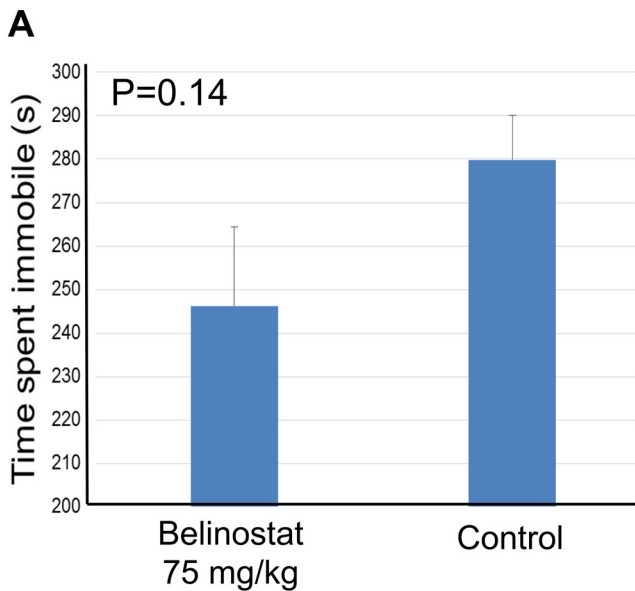
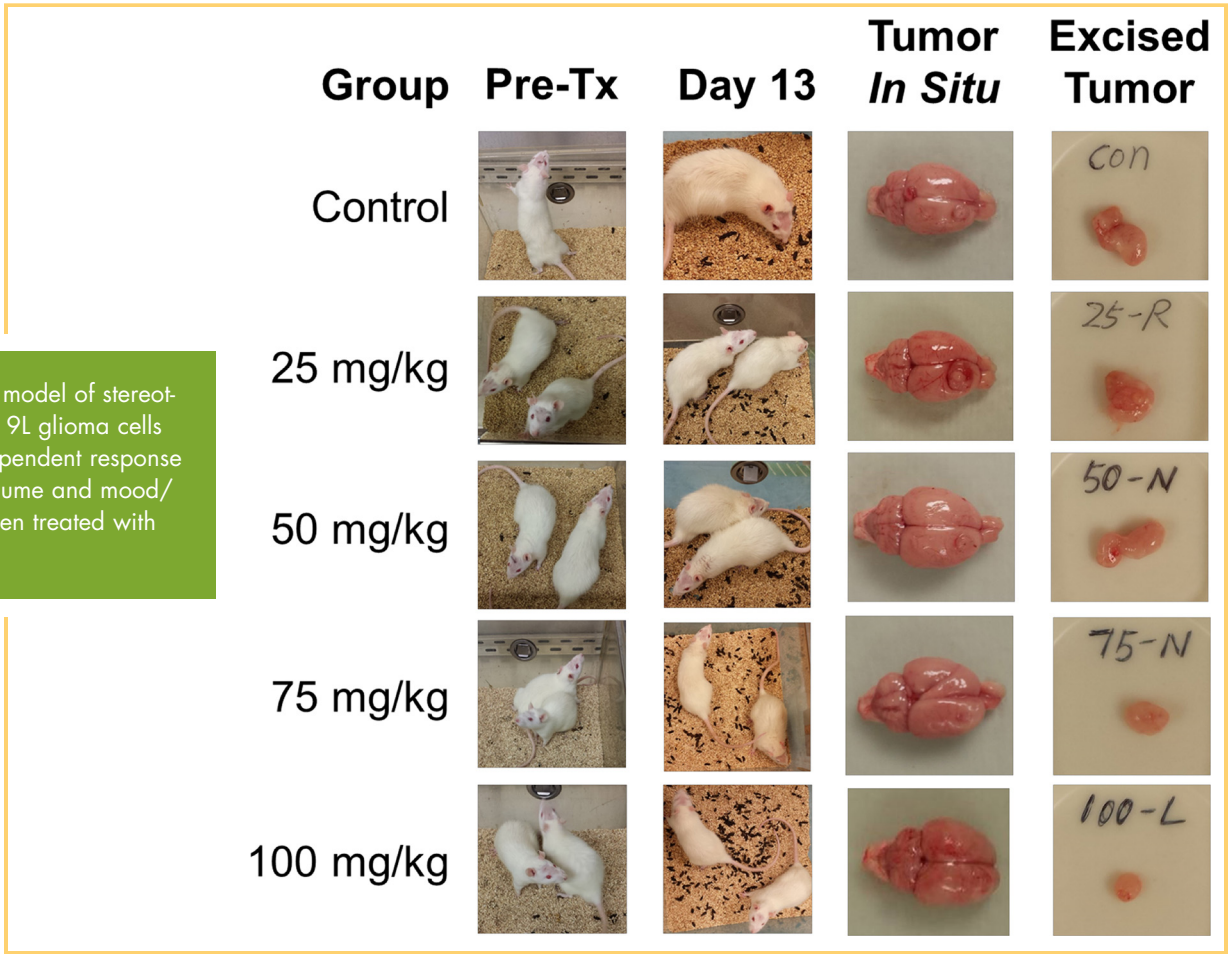


Figure 3. Two mouse models of depression to assess antidepressive effect of belinostat: Force-swim test measuring the time spent in immobility during 2–8 minutes (6 minutes) (A). Tail suspension test measuring the time spent in immobility in mice treated with lipopolysaccharide (LPS) for 6 minutes. Five mice were used in each group (B).

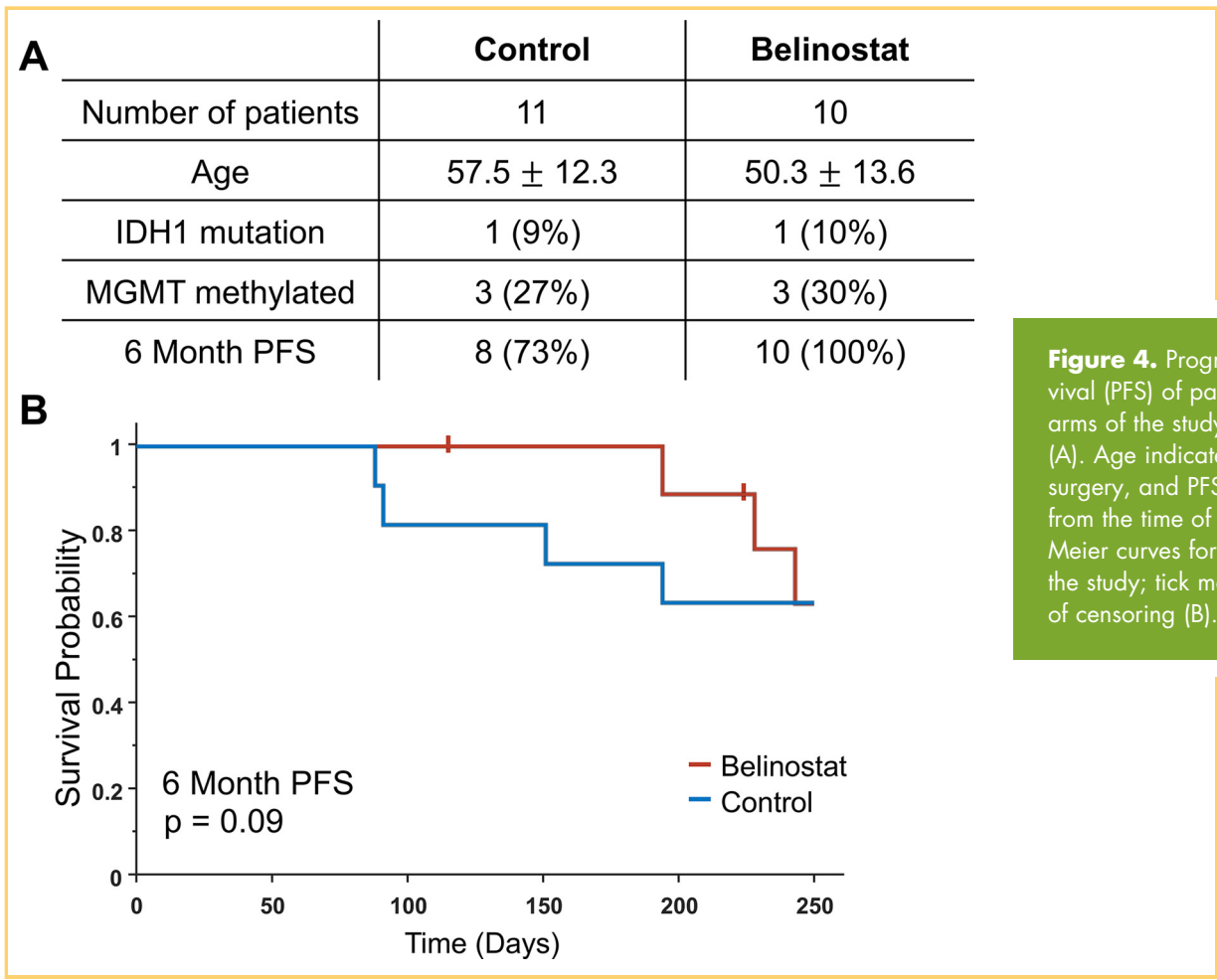


Figure 4. Progression-free survival (PFS) of patients in both arms of the study up to 1 year (A). Age indicates age at time of surgery, and PFS is right-censored from the time of surgery. Kaplan-Meier curves for the 2 arms of the study; tick marks indicate time of censoring (B).

Antidepressant Effect of Belinostat in 2 Animal Models

Figure 3 shows the results of the forced-swim and tail suspension tests. In the forced-swim test, the mice who received belinostat spent less time immobile compared to the control mice ($P = .14$). In the tail suspension test, the mice who received LPS + belinostat had a statistically significant decrease in immobility compared with mice who received LPS alone ($P = .02$).

In Vitro Study of mRNA Expression

mRNA expression levels of MIP (a bottleneck enzyme in the production of MI) from HDACi-treated cells are shown in online Supplemental Figure 2 as fold-increases in log-scale compared with those of the untreated cells (DMSO vehicle control). Belinostat showed greater increases in restoration of mRNA levels at the same concentration as other HDACi, including SAHA. The only other HDACi which achieved greater efficacy is quisinostat (JNJ26481585, Janssen Pharmaceuticals, Beerse, Belgium), a second-generation pan-HDACi, which was being tested in phase II clinical trials for multiple myeloma (23). However, currently there are no active trials for quisinostat on ClinicalTrials.gov.

Clinical Study

In total, 21 patients who met inclusion criteria for analysis were assessed to determine differences in PFS between the 2 arms (see online Supplemental Figure 1). A table summarizing basic demographics of the 2 arms of the clinical study is shown in Figure 4A. Both arms showed similar distributions of known genetic

targets that improve response to radiation—mutation of isocitrate dehydrogenase 1 (IDH1) and promoter methylation of the gene for O (6)-methylguanine-DNA methyltransferase (24). Figure 4B shows Kaplan-Meier curves for PFS from date of surgery (tick marks indicate time of censoring). Six-month PFS was 73% for the control arm and 100% for the belinostat arm. A log-rank test assessing PFS data up to 6 months trended toward statistical significance ($P = .09$). No statistically significant difference was observed on a log-rank test assessing PFS data up to 12 months ($P = .45$). Of these 21 patients, 17 completed an IDS-SR survey at both baseline (week 0 for belinostat arm, week

Table 1. IDS-SR Assessment

	Control	Belinostat	P value
Number of Patients	10	7	
Baseline Score	18.2 ± 9.1	22.0 ± 9.8	0.43
Week 11 Score	22.3 ± 10.9	16.1 ± 15.5	0.39
Change in Score	4.1 ± 9.7	-5.9 ± 8.7	0.04

The IDS-SR assessment of patients in both study arms between baseline and 1-month post-RT shows a statistically significant improvement in assessment scores for patients who received belinostat. P values indicate results of a two-tailed unpaired t -test.

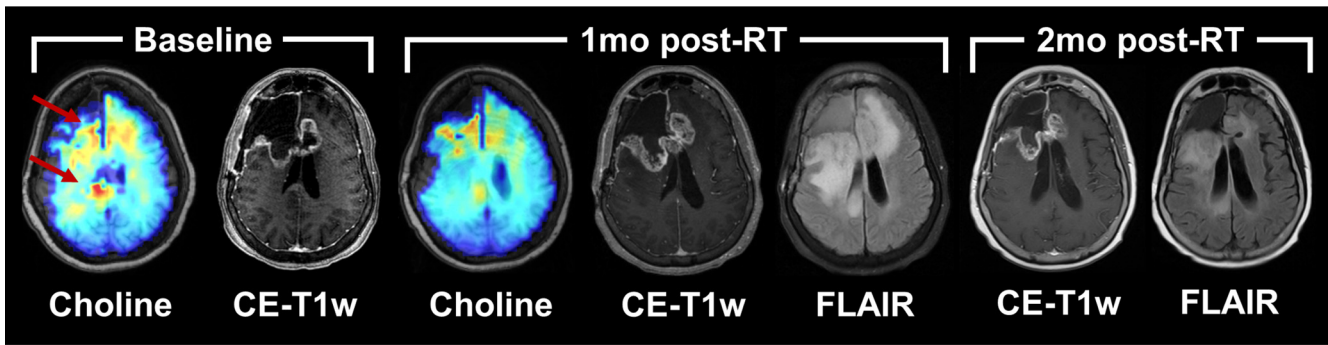


Figure 5. Longitudinal imaging of a patient in the control arm of the study. An sMRI map of choline indicates a response to chemoradiation between baseline and the first follow-up; however, standard clinical imaging indicates potential progression of disease. Further follow-up indicates that the imaging findings at 1 month were attributable to pseudoprogession.

1 for control arm) and at week 11 (see online Supplemental Figure 2; Table 1). While no significant difference in the scores was observed at either time point, the belinostat cohort had a statistically significant improvement in scores over the course of treatment using a 2-tailed unpaired *T* test ($P = .04$).

Figures 5 and 6 depict sMRI and clinical CE-T1w MRI scans for 2 representative patients, 1 from each of the study arms. At baseline, both patients showed elevated choline metabolism (red arrows) around the resection cavities, indicating the presence of increased cellular turnover associated with neoplasia. One-month post-RT (week 11), both patients showed decreased levels of choline compared with baseline, and low NAA levels owing to subsequent radiation damage to in-field neurons. Therefore, Cho/NAA did not reliably indicate early response (see online Supplemental Figure 3); however, we found that peritumoral MI

was improved in the subject who received belinostat (see online Supplemental Figure 3) at 1-month post-RT. The control patient (Figure 5) was deemed to have potential progression of her disease because of the thickened contrast enhancement around the resection cavity on CE-T1w imaging; a month later, however, the thickened contrast rim was gone, and the patient was deemed to not yet have disease progression. The patient in the belinostat arm (Figure 6) had a similar course; only the increase in enhancement occurred 3 months after radiation was completed.

DISCUSSION

In this work, we sought to characterize the antitumor and antidepressant activity of belinostat, a new HDACi with improved brain penetration, in a translational manner: starting from in

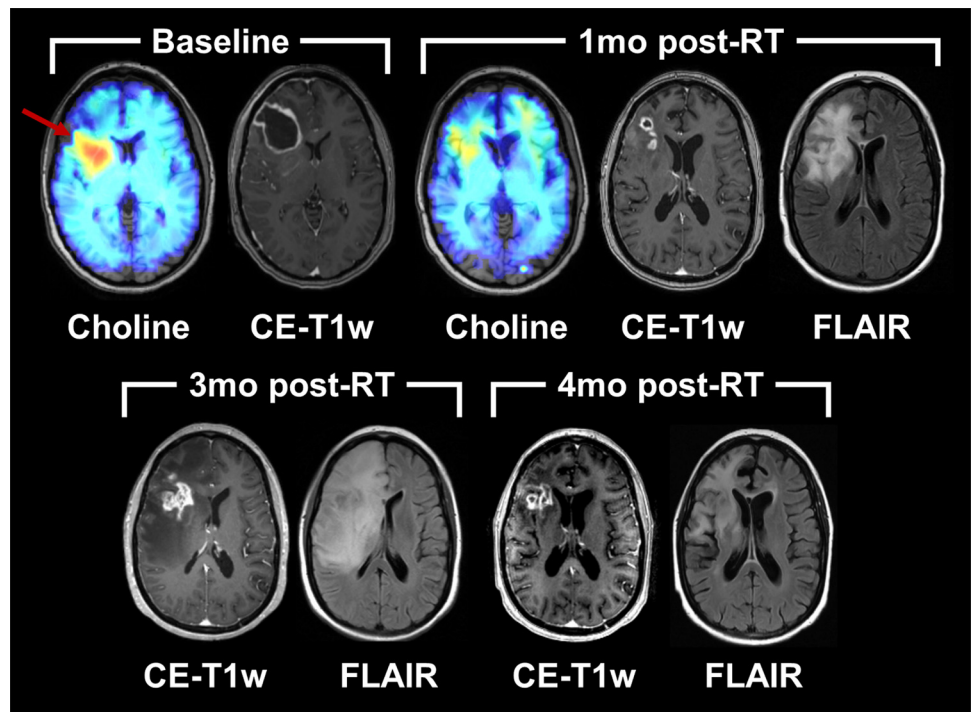


Figure 6. Longitudinal imaging of a patient in the belinostat (treatment) arm of the study. An sMRI map of choline indicates a response to chemoradiation as assessed at 1 month post-RT. Additional follow-up imaging indicates the pseudoprogession phenomenon occurring at 3 month post-RT, resolving by 4 month post-RT.

vivo animal glioma models to testing in patients with glioblastoma. First, we assessed the efficacy of belinostat in reducing tumor volume in an orthotopic rat glioma model. Here, a dose-dependent reduction in tumor size was observed, suggesting the antitumor properties of the drug are effective in crossing the blood–brain barrier in vivo (Figure 2). In addition, it was observed that the activity levels of rats, as measured by grooming activities and droppings, were higher in those treated with increased doses of belinostat. These improvements are consistent with previously reported literature by Covington et al. (25) that HDACis possess antidepressant properties. To further assess the antidepressive effect of belinostat, we subjected mice to 2 different models of induced depression. We found that belinostat reduced the immobility time in both the forced-swim and tail suspension tests (Figure 3), exhibiting the drug's antidepressant effect. We followed these tests with an in vitro assessment of belinostat's effect on MIP, the key enzyme in the production of MI that was implicated in depression. The in vitro cell study showed that belinostat had greater restorative activity for MIP than most other HDACi. An HDACi tested that had higher restoration than belinostat was quisinostat (JNJ26481585); however, there is no clinical trial currently enrolling patients testing quisinostat. As such, belinostat shows promise as a targeted HDACi for glioblastoma because of its increased uptake into the brain and its efficacy in restoring key metabolic activity for depression.

The belinostat clinical trial completed enrollment of patients in August 2018, and patients are continuing to be followed to assess long-term outcomes including progression-free and overall survival. Although statistical claims cannot yet be made regarding long-term survival and efficacy, a comparison of 6-month PFS and initial changes in mood are presented in this work. The cohort receiving belinostat showed a trend of improved 6-month PFS compared to the control cohort ($P = .09$); however, this difference was mitigated by 12 months ($P = .45$). Despite a limited sample size for this study, these results suggest that belinostat may improve response to chemoradiation therapy as hypothesized. A speculated reason for the improved PFS at 6 months but not at 12 months is that belinostat was given to subjects for only a short term during RT.

While 6-month PFS outcomes approached statistical significance, the belinostat cohort did achieve a statistically significant improvement in depression as measured by the IDS-SR ($P = 0.04$). This suggests that the mood improvement effect of belinostat, as shown in our animal data and with the claim by Covington et al. (25), may translate to humans. These preliminary data suggest future large cohorts to be evaluated.

Finally, this study showed the potential of sMRI as a non-invasive monitoring tool for investigational therapeutics. As

shown in Figures 5 and 6, both patients appeared to have a reduced tumor burden when assessing choline metabolism at week 1, 1 month after the completion of RT. Owing to radiation-induced damage, NAA was reduced around the high dose area, which made Cho/NAA ineffective in assessing tumor response (see online Supplemental Figure 3). MI showed a slight improvement back towards normal level at the 1-month post-RT scan in the patient treated with belinostat, consistent with IDS-SR score improvement (see online Supplemental Figure 3). Further studies, including longitudinal scanning, are needed to fully elucidate the timeline of metabolite changes in these patients. Standard imaging, however, differed between the 2 patients and suggested that the control patient may have been experiencing disease progression, when eventually it turned out to be stable disease at that time. This is a phenomenon known as pseudoprogression, the ambiguity of CE-T1w findings in differentiating true progression of disease from normal tissue response to high-dose radiation. sMRI, however, is robust to the pseudoprogression phenomenon, as the modality is measuring endogenous intracellular metabolism rather than vasculature damages/changes or tissue phenomena such as edema. Both patients showed similar metabolic signatures, which turned out to be more accurate of the underlying pathology compared to clinical imaging.

CONCLUSION

In this work we described the therapeutic and antitumor, anti-depression effects of belinostat, a potent pan-HDACi with blood–brain barrier permeability through: a rat glioma model, 2 mouse depression models, an in vitro cell study, and testing in a pilot clinical study in patients with glioblastoma. The results from this work suggest that belinostat may be an effective HDACi at delaying disease progression and improving depression. Furthermore, it shows that the treatment response can be monitored noninvasively using spectroscopic MRI during pseudoprogression period. Further studies and analysis of the ongoing clinical trial may yield a better understanding of the role that HDACis play in the metabolic profiles of GBM and motivate the development of better, targeted therapies for patients with this debilitating disease.

Additional testing of this drug in human subjects can help with separating this improved mood/activity effect due to a primary property of HDACis from improvement as a secondary effect to reduced tumor burden.

Supplemental Materials

Supplemental Figure 1-3: <http://dx.doi.org/10.18383/j.tom.2018.00031.sup.01>

ACKNOWLEDGMENTS

We would like to thank Spectrum Pharmaceuticals for providing the investigational drug used in this clinical study; the staff at the Clinical Trials Office at the Winship Cancer Institute for their support and assistance with recruiting and managing the patients enrolled in the clinical study; and Dr. Andrew Maudsley and Mr. Sulaiman Sheriff at the University of Miami for their support with the EPSI sequence and MIDAS software framework. Funding for this work came from National Institutes of Health grant U01CA172027.

Disclosures: No disclosures to report.

Conflict of Interest: The authors have no conflict of interest to declare.

REFERENCES

- Stupp R, Taillibert S, Kanner AA, Kesari S, Steinberg DM, Toms SA, Taylor LP, Lieberman F, Silvani A, Fink KL, Barnett GH, Zhu JJ, Henson JW, Engelhard HH, Chen TC, Tran DD, Sroubek J, Tran ND, Hottinger AF, Landolfi J, Desai R, Caroli M, Kew Y, Honnorat J, Idbaih A, Kirson ED, Weinberg U, Pali Y, Hegi ME, Ram Z. Maintenance therapy with tumor-treating fields plus temozolomide vs temozolomide alone for glioblastoma: a randomized clinical trial. *JAMA*. 2015;314:2535–2543.
- Minucci S, Pelicci PG. Histone deacetylase inhibitors and the promise of epigenetic (and more) treatments for cancer. *Nat Rev Cancer*. 2006;6:38–51.
- Cornago M, Garcia-Alberich C, Blasco-Angulo N, Vall-Laura N, Nager M, Herreros J, Comella JX, Sanchis D, Llovera M. Histone deacetylase inhibitors promote glioma cell death by G2 checkpoint abrogation leading to mitotic catastrophe. *Cell Death Dis*. 2014;5:e1435.
- Mottamal M, Zheng S, Huang TL, Wang G. Histone deacetylase inhibitors in clinical studies as templates for new anticancer agents. *Molecules*. 2015;20:3898–3941.
- Bieliauskas AV, Pflum MKH. Isoform-selective histone deacetylase inhibitors. *Chem Soc Rev*. 2008;37:1402–1413.
- Falkenberg KJ, Johnstone RW. Histone deacetylases and their inhibitors in cancer, neurological diseases and immune disorders. *Nat Rev Drug Discov*. 2014;13:673–691.
- Mann BS, Johnson JR, Cohen MH, Justice R, Pazdur R. FDA approval summary: vorinostat for treatment of advanced primary cutaneous T-cell lymphoma. *Oncologist*. 2007;12:1247–1252.
- Wei L, Hong S, Yoon Y, Hwang SN, Park JC, Zhang Z, Olson JJ, Hu XP, Shim H. Early prediction of response to Vorinostat in an orthotopic rat glioma model. *NMR Biomed*. 2012;25:1104–1111.
- Eyüpoglu IY, Hahnen E, Buslei R, Siebzehnrübl FA, Savaskan NE, Lüders M, Tränkle C, Wick W, Weller M, Fahlbusch R, Blümcke I. Suberoylanilide hydroxamic acid (SAHA) has potent anti-glioma properties in vitro, ex vivo and in vivo. *J Neurochem*. 2005;93:992–999.
- Krauze AV, Myrehaug SD, Chang MG, Holdford DJ, Smith S, Shih J, Tofilon PJ, Fine HA, Camphausen K. A phase 2 study of concurrent radiation therapy, temozolomide, and the histone deacetylase inhibitor valproic acid for patients with glioblastoma. *Int J Radiat Oncol Biol Phys*. 2015;92:986–992.
- Wang C, Eessalu TE, Barth VN, Mitch CH, Wagner FF, Hong Y, Neelamegam R, Schroeder FA, Holson EB, Haggarty SJ, Hooker JM. Design, synthesis, and evaluation of hydroxamic acid-based molecular probes for in vivo imaging of histone deacetylase (HDAC) in brain. *Am J Nucl Med Mol Imaging*. 2013;4:29–38.
- Hanson JE, LA H, Plise E, Chen Y-H, Ding X, Hania T, Sabath EV, Alexandrov V, Brunner D, Leahy E, Steiner P, Liu L, Searce-Levie K, Zhou Q. SAHA enhances synaptic function and plasticity in vitro but has limited brain availability in vivo and does not impact cognition. *PLoS One*. 2013;8:e69964.
- Lee H-Z, Kwitkowski VE, Del Valle PL, Ricci MS, Saber H, Habtemariam BA, Bullock J, Bloomquist E, Li Shen Y, Chen XH, Brown J, Mehrotra N, Dorff S, Charlab R, Kane RC, Kaminskas E, Justice R, Farrell AT, Pazdur R. FDA Approval: Belinostat for the Treatment of Patients with Relapsed or Refractory Peripheral T-cell Lymphoma. *Clin Cancer Res*. 2015;21:2666–2670.
- Liang Z, Wu H, Xia J, Li Y, Zhang Y, Huang K, Wagar N, Yoon Y, Cho HT, Scala S, Shim H. Involvement of miR-326 in chemotherapy resistance of breast cancer through modulating expression of multidrug resistance-associated protein 1. *Biochem Pharmacol*. 2010;79:817–824.
- Krishnan R, Cella D, Leonardi C, Papp K, Gottlieb AB, Dunn M, Chiou CF, Patel V, Jahreis A. Effects of etanercept therapy on fatigue and symptoms of depression in subjects treated for moderate to severe plaque psoriasis for up to 96 weeks. *Br J Dermatol*. 2007;157:1275–1277.
- Cryan JF, Mombereau C, Vassout A. The tail suspension test as a model for assessing antidepressant activity: review of pharmacological and genetic studies in mice. *Neurosci Biobehav Rev*. 2005;29:571–625.
- O'Connor JC, Lawson MA, Andre C, Moreau M, Lestage J, Castanon N, Kelley KW, Dantzer R. Lipopolysaccharide-induced depressive-like behavior is mediated by indoleamine 2, 3-dioxygenase activation in mice. *Mol Psychiatry*. 2009;14:511–522.
- Burnet NG, Thomas SJ, Burton KE, Jefferies SJ. Defining the tumour and target volumes for radiotherapy. *Cancer Imaging*. 2004;4:153–161.
- Maudsley A, Domenig C. Signal normalization for MR spectroscopic imaging using an interleaved water-reference. *Int Soc Magn Reson Med*. 2009;61:548–559.
- Maudsley AA, Domenig C, Govind V, Darkazanli A, Studholme C, Arheart K, Bloomer C. Mapping of brain metabolite distributions by volumetric proton MR spectroscopic imaging (MRSI). *Magn Reson Med*. 2009;61:548–559.
- Rush AJ, Carmody T, Reimnitz PE. The Inventory of Depressive Symptomatology (IDS): clinician (IDS-C) and self-report (IDS-SR) ratings of depressive symptoms. *Int J Methods Psychiatr Res*. 2000;9:45–59.
- Rush AJ, Gullion CM, Basco MR, Jarrett RB, Trivedi MH. The inventory of depressive symptomatology (IDS): psychometric properties. *Psychol Med*. 1996;26:477–486.
- Moreau P, Facon T, Touzeau C, Benboubker L, Delain M, Badamo-Dotzis J, Phelps C, Doty C, Smit H, Fourneau N, Forslund A, Hellemans P, Leleu X. Quisinstat, bortezomib, and dexamethasone combination therapy for relapsed multiple myeloma. *Leuk Lymphoma*. 2016;57:1546–1559.
- Stupp R, Hegi ME, Mason WP, van den Bent MJ, Taphoorn MJB, Janzer RC, Ludwin SK, Allgeier A, Fisher B, Belanger K, Hau P, Brandes AA, Gijtenbeek J, Marosi C, Vecht CJ, Mokhtari K, Wesseling P, Villa S, Eisenhauer E, Gorlia T, Weller M, Lacombe D, Cairncross JG, Mirimanoff RO; European Organisation for Research and Treatment of Cancer Brain Tumour and Radiation Oncology Groups; National Cancer Institute of Canada Clinical Trials Group. Effects of radiotherapy with concomitant and adjuvant temozolomide versus radiotherapy alone on survival in glioblastoma in a randomised phase III study: 5-year analysis of the EORTC-NCIC trial. *Lancet Oncol*. 2009;10:459–466.
- Covington HE, 3rd, Maze I, LaPlant QC, Vialou VF, Ohnishi YN, Berton O, Fass DM, Renthall W, Rush AJ 3rd, Wu EY, Ghose S, Krishnan V, Russo SJ, Tamminga C, Haggarty SJ, Nestler EJ. Antidepressant actions of histone deacetylase inhibitors. *J Neurosci*. 2009;29:11451–1160.